



Published in final edited form as:

*ACS Chem Neurosci.* 2023 August 16; 14(16): 2827–2829. doi:10.1021/acchemneuro.3c00482.

## TMEM106B Fibrils from FTLD Patients and Healthy Controls

**James D. Greenwood,**

Department of Chemistry, University of Colorado, Boulder, Colorado 80309, United States

**Wyatt C. Powell,**

Department of Chemistry, University of Colorado, Boulder, Colorado 80309, United States

**Maciej A. Walczak**

Department of Chemistry, University of Colorado, Boulder, Colorado 80309, United States

### Abstract

Recent studies involving four research teams have revealed that amyloid fibrils in FTLD-TDP patients and cognitively healthy individuals primarily consist of TMEM106B, a protein previously identified as a risk factor for FTLD-TDP. Through cryogenic electron microscopy, the studies identified various protofilament structures of TMEM106B fibrils from individuals with several neurodegenerative diseases. These findings raise new questions and opportunities for future research, as they suggest that TMEM106B plays a central role in FTLD pathology. These discoveries also prompt the need for the development of specific antibodies for fibrillar TMEM106B and necessitate further investigation of the potential mechanistic link between TMEM106B and other filamentous aggregates. The power of cryo-EM techniques is underscored in these unexpected findings and may be a vital tool for gaining further molecular insights into neurodegenerative diseases characterized by amyloid deposits.

### Keywords

FTLD-TDP; amyloid fibrils; TMEM106B; FTLD pathology; filamentous aggregates; amyloid deposits

---

Frontotemporal lobar degeneration (FTLD), the third most prevalent neurodegenerative disease, primarily affects individuals aged 45–60 years. Patients typically exhibit behavioral changes and diminished language abilities. Interestingly, about 50% of FTLD cases feature neuronal inclusions of the TAR DNA-binding protein (TDP-43), defining the subset known as FTLD-TDP. Despite the clinical significance of TDP-43 deposits, a comprehensive understanding of their nature remains elusive. Recently, four research teams reported that both amyloid fibrils from FTLD-TDP patients and those from cognitively healthy individuals consisted of TMEM106B, a protein previously associated with FTLD-TDP risk. These teams studied sarkosyl-insoluble fractions using negative stain transmission electron microscopy and cryogenic electron microscopy (cryo-EM), achieving structures

---

**Corresponding Author Maciej A. Walczak** – maciej.walczak@colorado.edu.

Complete contact information is available at: <https://pubs.acs.org/10.1021/acchemneuro.3c00482>

The authors declare no competing financial interest.

with resolutions up to 2.9 Å. Initially, researchers expected to find TDP-43 as the primary protein candidate. However, this hypothesis was invalidated due to poor electron density match in the models. Instead, the densities corresponded to the proteolytic fragment of TMEM106B.

In the Eisenberg study, amyloid fibrils were found in 38 out of 40 donors with confirmed types A, B, C, and D FTLN-TDP (Figure 1).<sup>1</sup> Fibrils were extracted from one brain sample from each FTLN-TDP type and imaged with cryo-EM. They discovered three protofilament polymorphs, all sharing a common fold. One fibril consisted of a single protofilament, while the others were paired. The interface in the more prevalent paired fibril was mediated by residues K178 and R180 of each protofilament interacting with an unresolved density, potentially an anionic cofactor. No fibrils were found in the eight non-FTLN-TDP control samples.

The Scheres group obtained cryo-EM structures of TMEM106B fibrils from 22 individuals with various neurodegenerative diseases, including Alzheimer's disease (AD), dementia with Lewy bodies (DLB), Parkinson's disease (PD), progressive supranuclear palsy (PSP), and corticobasal degeneration (CBD).<sup>2</sup> They identified three different protofilament folds, with the N-terminal region (S120-T166) adopting the same conformation in each. Each protofilament fold type appeared in both single and paired fibrils. However, only one paired fibril structure was solved. The interprotofilament interface mirrored that found by Eisenberg's group, with residues K178 and R180 on each protofilament as well as an unresolved density. There was no observed correlation between fibril folds and specific diseases. While fibrils were detected in three elderly, neurologically normal individuals, none were found in samples from younger, neurologically normal individuals.

Led by the Fitzpatrick group, the study found two TMEM106B protofilament folds in brain tissue from eight FTLN-TDP patients, two PSP patients, and one DLB patient.<sup>3</sup> One fold was discovered in both single and paired protofilament fibrils. This fold closely resembled those found by Eisenberg's and Scheres' groups, including the unresolved anionic cofactor mediating the K178/R180 interface. Notably, in both the Fitzpatrick and Scheres studies, TMEM106B fibrils were also found in patients with tauopathies and  $\alpha$ -synucleinopathies.

Finally, the study by the Jiang group characterized TMEM106B amyloid filaments from the gray and the white matter, which were identical in both samples.<sup>4</sup> The protofilament core of TMEM106B includes residues 120–254 and 17  $\beta$ -strands depicted in Figure 1.

TMEM106B is a transmembrane protein which is expressed primarily in neurons and oligodendrocytes, where it is localized in late endosome/lysosome compartments. It is composed of 274 amino acids in which residues 1–96 are cytoplasmic, amino acids 97–117 comprise a single-pass helical transmembrane domain, and residues 118–274 are luminal (Figure 2). With an estimated molecular weight of 31 kDa, TMEM106B shows on a gel at ~43 kDa due to extensive glycosylation. Overexpression of TMEM106B in various cell lines (including neurons) results in lysosome enlargement and causes cell death and cytotoxicity. TMEM106B forms homodimers and heterodimers with its homolog TMEM106C although the physiological role of dimerization is poorly understood the moment. Cathepsins D4 and

other lysosomal proteases cleave TMEM106B into the transmembrane and intracellular domains, which are further processed into smaller fragments by the GxGD aspartyl proteases SPPL2a. At the moment, the potential biological role of smaller fragments of TMEM106B remain to be tested, and likely these functions can be controlled by protein glycosylation. TMEM106B controls lysosomal pH by interacting with V-ATPase accessory protein 1 (AP1) and AP2M, while TMEM106B deficiency impairs lysosomal acidification.

As a lysosomal protein, TMEM106B undergoes significant N-glycosylation.<sup>5</sup> Haass proposed five glycosylation sites (N145, N151, N164, N183, N256) through site mutagenesis, and the presence of four glycans in the ordered fibril core was confirmed by cryo-EM structures. All these glycosylations, consistent with the canonical biosynthesis pathway of mammalian glycoproteins, are located within the Asn-Xaa-Thr/Ser consensus sequence. Treatment of TMEM106B with endoglycosidase F (EndoF) revealed that the protein contains N-linked glycans of complex type, as this enzyme only removes N-linked glycans of complex type. The treatment resulted in bands ~11 kDa lower than the molecular weight of TMEM106B, suggesting the presence of biantennary glycans. However, their precise structure, topology, and the presence of sialic acids still need to be elucidated. Simple glycan modifications are added at the first three N-glycosylation sites on mature TMEM106B, while complex glycans are detected at the last two sites. TMEM106B is partially resistant to endoglycosidase H, suggesting its transport to late secretory compartments and the absence of high mannose glycans.

From a clinical perspective, TMEM106 recently gained substantial interest because it was identified as a risk factor for FTLD-TDP in patients with GRN (progranulin gene) mutations. Furthermore, TMEM106b can also serve as a receptor for SARS-CoV-2 entry into angiotensin-converting enzyme 2 (ACE2)-negative cells.<sup>6</sup> Overexpression of TMEM106B leads to increased progranulin (PGRN) levels, reduces processing of PRGN into granulin peptides, and may disrupt the endosomal-lysosomal trafficking of PRGN. A GWAS study identified multiple SNPs within a 68 kb region on chromosome 7p21 that were associated with the occurrence of FTLD-TDP. The rs3173615 variant in TMEM106B is a coding SNP resulting in a Thr to Ser change at amino acid 185. This mutation is associated with attenuated cognitive deficits and improved cognitive performance in several diseases such as presymptomatic FTLD, ALS, and other neuropathological conditions. The TMEM106B risk haplotype (rs3173615 TT) is also linked to reduced expression of neuronal markers and increased expression of inflammatory genes in neuropathologically normal older individuals. The current understanding is that the S185 allele confers neuronal protection and is associated with faster protein degradation than the T185 allele.

Overall, the structural studies open several important questions regarding the pathology of FTLD and highlight possible future research directions. Immunostaining of patient-extracted fibrils with known TMEM106B antibodies yielded no positive results, likely because these antibodies recognize epitopes that are cleaved off before the fibrils are assembled or are inaccessible within the core. More work is needed to develop antibodies specific for fibrillar TMEM106B or the C-terminal residues accessible in the fuzzy coat region, which could improve diagnostic accuracy. In addition, it would be interesting to determine whether TDP-43 aggregates, which can be coextracted with TMEM106B fibrils from patients with

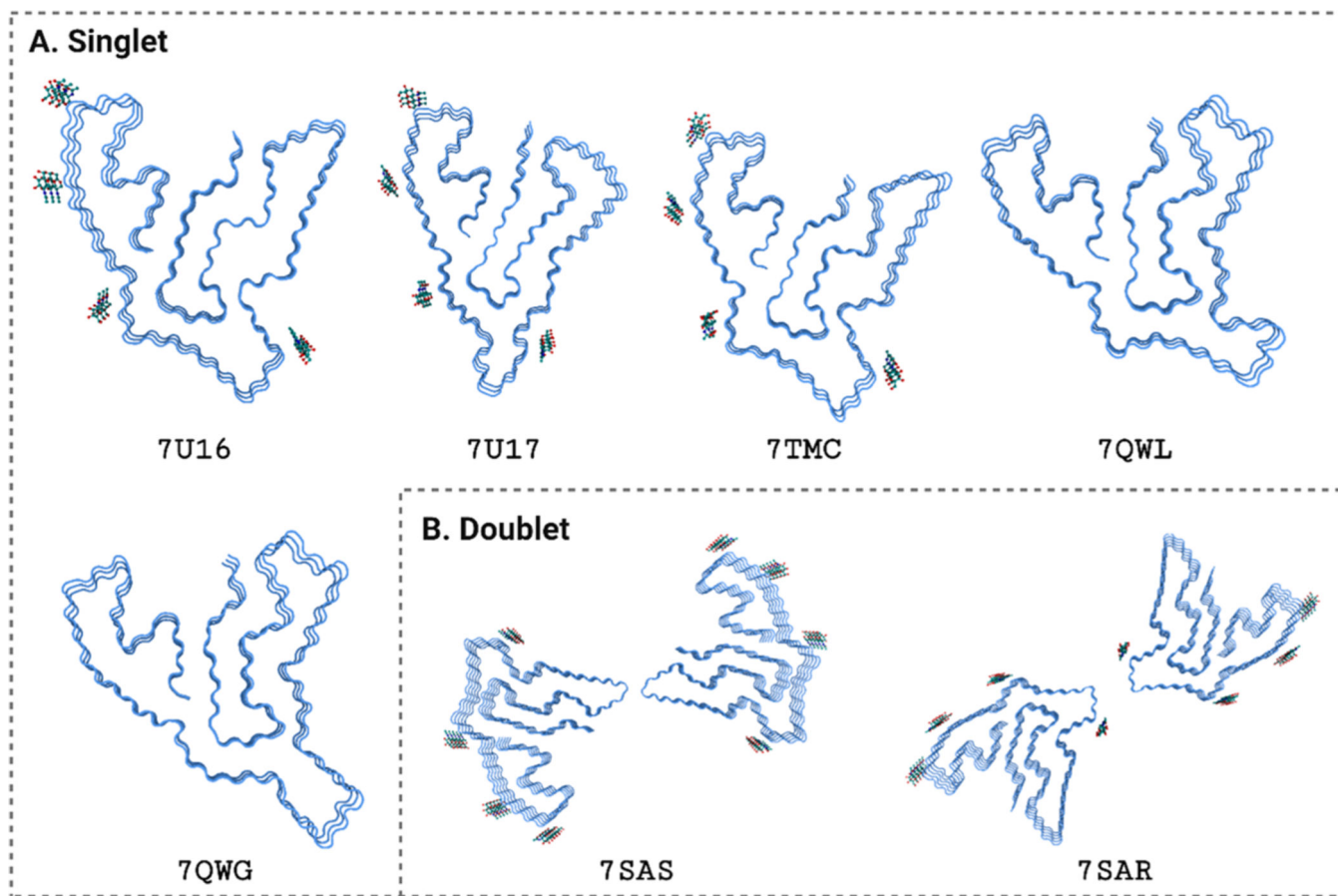
FTLD-TDP, colocalize with TMEM106B in the human brain or if there is a mechanistic link (e.g., cross-seeding) between TMEM106B and other filamentous aggregates. These unexpected discoveries underscore the power of cryo-EM techniques and can provide molecular insights into neurodegenerative diseases characterized by amyloid deposits.

## ACKNOWLEDGMENTS

This work was supported by the National Institute on Aging (Grant RF1AG079294) and the University of Colorado Boulder. Figure 1 was created with [biorender.com](https://biorender.com).

## REFERENCES

- (1). Jiang YX; Cao Q; Sawaya MR; Abskharon R; Ge P; DeTure M; Dickson DW; Fu JY; Ogorzalek Loo RR; Loo JA; Eisenberg DS *Nature* 2022, 605, 304–309. [PubMed: 35344984]
- (2). Schweighauser M; Arseni D; Bacioglu M; Huang M; Lövestam S; Shi Y; Yang Y; Zhang W; Kotecha A; Garringer HJ; Vidal R; Hallinan GI; Newell KL; Tarutani A; Murayama S; Miyazaki M; Saito Y; Yoshida M; Hasegawa K; Lashley T; Revesz T; Kovacs GG; van Swieten J; Takao M; Hasegawa M; Ghetti B; Spillantini MG; Ryskeldi-Falcon B; Murzin AG; Goedert M; Scheres SHW *Nature* 2022, 605, 310–314. [PubMed: 35344985]
- (3). Chang A; Xiang X; Wang J; Lee C; Arakhamia T; Simjanoska M; Wang C; Carlomagno Y; Zhang G; Dhingra S; Thierry M; Perneel J; Heeman B; Forgrave LM; DeTure M; DeMarco ML; Cook CN; Rademakers R; Dickson DW; Petrucelli L; Stowell MHB; Mackenzie IRA; Fitzpatrick AWP *Cell* 2022, 185, 1346–1355. [PubMed: 35247328]
- (4). Hoq MR; Bharath SR; Hallinan GI; Fernandez A; Vago FS; Ozcan KA; Li D; Garringer HJ; Vidal R; Ghetti B; Jiang W. *Acta Neuropathol.* 2023, 145, 707–710. [PubMed: 36952000]
- (5). Lang CM; Fellerer K; Schwenk BM; Kuhn PH; Kremmer E; Edbauer D; Capell A; Haass C. *J. Biol. Chem* 2012, 287, 19355–19365. [PubMed: 22511793]
- (6). Baggen J; Jacquemyn M; Persoons L; Vanstreels E; Pye VE; Wrobel AG; Calvaresi V; Martin SR; Roustan C; Cronin NB; Reading E; Thibaut HJ; Vercruyse T; Maes P; De Smet F; Yee A; Nivitchanyong T; Roell M; Franco-Hernandez N; Rhinn H; Mamchak AA; Ah Young-Chapon M; Brown E; Cherepanov P; Daelemans D. *Cell* 2023, DOI: 10.1016/j.cell.2023.06.005.

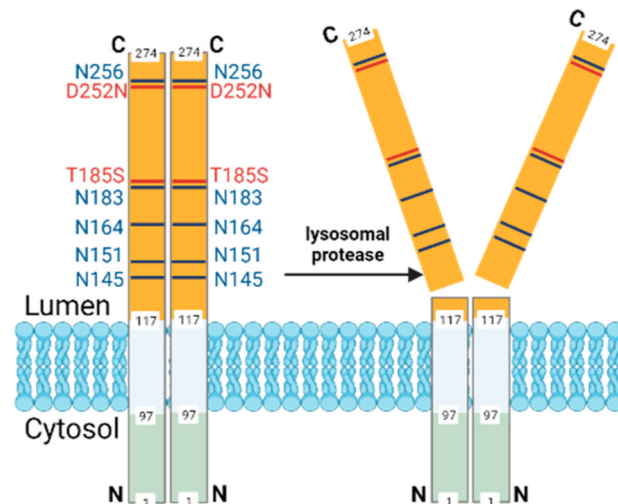


**Figure 1.** Summary of cryo-EM structures classified as singlets and doublets. Structure designations refer to PDB entries.

A.

10	20	30	40	50
MGKSLSHLPL	HSSKEDAYDG	VTSENMRNGL	VNSEVHNEDG	RNGDVSQFPY
60	70	80	90	100
VEFTGRDSVT	CPTCQGTGRI	PRGQ ENQLVA	LIPYSDQRLR	PRRTKLY VMA
110	120	130	140	150
SVFVCLLLSG	LAVFFLF PRS	IDVKYIGVKS	AYVSYDVQKR	TIYLNITNTL
160	170	180	190	200
NITNNNYYSV	EVENITAQVQ	FSKTVIGKAR	LNNITIIIGPL	DMKQIDYTPV
210	220	230	240	250
TVIAEEMSYM	YDFCTLISIK	VHNIVLMMQV	TVTTTYFGHS	EQISQERYQY
260	270			
VDCGRNTTYQ	LGQSEYLNVL	QPQQ		

B.

**Figure 2.**

(A) Primary sequence and (B) structural organization of TMEM106B and lysosomal processing (Uniprot Q9NUM4). Residues in blue depict confirmed N-linked glycosylation sites.